MULTIPLE DELAYED RESONATOR VIBRATION ABSORBERS FOR MULTI-DEGREE-OF-FREEDOM MECHANICAL STRUCTURES

N. JALILI

Department of Mechanical Engineering, Northern Illinois University, DeKalb, Illinois 60115-2854, *U.S.A*

N. OLGAC

Department of Mechanical Engineering, The University of Connecticut, Storrs, CT 06269-3139, *U.S.A.*

This study is on the use of multiple Delayed Resonators (DR) in suppressing tonal vibration of multi-degree-of-freedom mechanical structures. The DR is a recently introduced, actively tunable vibration absorber which converts a conventional passive absorber into a marginally stable resonator. This structure absorbs all the vibratory energy at its point of attachment. Control forces in the form of proportional acceleration feedback with variable gains and time delays are considered here. Attractive features of DR have already been demonstrated for single DR absorber cases. When excitation has multiple harmonics, multiple DRs can be used, each DR suppressing one of the harmonics. The stability assessment, however, becomes very complex in this case, due to the presence of unrelated time delays in the system. Therefore, a simpler situation is considered here; single harmonic excitation and multiple identical DRs acting on the system. A strategy called "Stability charts" is used not only to resolve the stability question but also to find out the tuning speed of the absorption. An example case of two identical DRs on a 3-DOF system is presented. The results demonstrate the feasibility of using multiple DR absorbers.

© 1999 Academic Press

1. INTRODUCTION

Dynamic vibration absorbers have been effectively used to remove undesirable oscillations from mechanical structures. The ground rule of vibration absorption is to properly "sensitize" the absorber substructure such that it becomes absorbent of the vibratory energy. If the excitation is tonal (i.e., pure harmonic), this "sensitization" can be done very efficiently by bringing the absorber to resonance at the excitation frequency.

In DR the absorber subsection is sensitized to the excitation frequency using a time delayed acceleration feedback (see Figure 1). It converts the dissipative passive absorber structure (Figure 1(a)) into a conservative (or marginally stable) one, i.e., a resonator (Figure 1(b)). This technique offers a number of
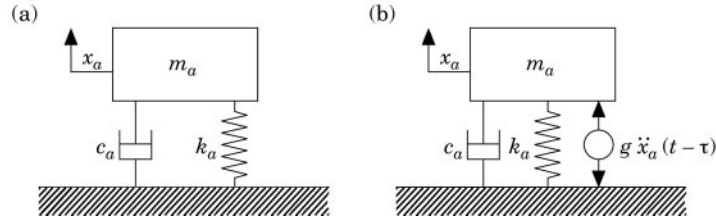
Figure 1. (a) The original passive absorber, (b) reconfigured dynamics, Delayed Resonator with acceleration feedback.

advantages: real time tunability, perfect tonal suppression, wide range of frequencies, simplicity of the control implementation, and robust design [1–6].

In earlier studies, the DR implementation was limited to suppressing vibrations at a single point of absorber attachment, on multi degree-of-freedom (MDOF) structures [4, 5, and 7]. When the objective is to quiet a number of locations on the system, multiple vibration absorbers are used. This study deals with multiple DR absorbers, and the issues associated with their design and implementation.

Typically, the time delay in a control loop is a destabilizing factor. As the DR absorber is tuned, the stability of the combined system (primary system equipped with the DR absorbers) should be assured. There is a fair amount of recent literature on the stability of delayed linear systems [3, 8–11]. These investigations consider only one delay or commensurate delays (i.e., integer multiples of one single delay). When the delays are totally unrelated, the analysis becomes very tedious. This would be the case for non-identical DR's trying to tune to single or multiple frequencies. Considering these difficulties, a simpler problem is proposed: multiple DR absorbers which have identical physical properties and the primary structure being excited by a single harmonic force.

Some design tools for the selection of the absorber parameters are also presented such that the desired absorption properties are achieved, in particular the absorber's tuning speed to time varying excitation frequencies. The text is composed as follows. The DR with acceleration feedback is briefly reviewed in section 2. Section 3 addresses the use of multiple identical DRs as vibration absorbers for MDOF structures. The governing equations of motion and the stability analysis are presented in this section. The parametric selection of the DR absorbers is addressed in section 4. The numerical results and simulations are given in section 5. Section 6 concludes the study and suggests some future research.

2. THE DELAYED RESONATOR CONCEPT

A brief overview of DR is presented here for clarity. The equation of motion governing the absorber dynamics (Figure 1(b)) is

$$m_a \ddot{x}_a(t) + c_a \dot{x}_a(t) + k_a x_a(t) - g \ddot{x}_a(t - \tau) = 0, \qquad (1)$$

where the last term represents the delayed acceleration feedback. The Laplace domain representation of this equation yields the characteristic equation

$$m_a s^2 + c_a s + k_a - g s^2 \mathrm{e}^{-\tau s} = 0. \tag{2}$$

Without feedback ($g = 0$) this structure is dissipative with two characteristic roots (poles) on the left half of the complex plane. For g and $\tau > 0$, however, these two finite stable roots are supplemented by infinitely many additional finite roots. Note that these characteristic roots (poles) of equation (2) are discretely located on $s = a + \mathrm{j}\omega$, and the following relation holds:

$$g = (\| m_a s^2 + c_a s + k_a \| / \| s^2 \|)\mathrm{e}^{\tau a}, \tag{3}$$

where $\| \cdot \|$ denotes the magnitude of the argument.

Using equation (3), the following observation can be made:

$g = 0:$ there are two finite stable poles and all remaining poles are at

$\qquad\qquad a = -\infty,$

$g = +\infty:$ there are two poles at $s = 0$, and the rest are at $a = +\infty$.   (4)

Considering these observations and taking into account the continuity of the root loci for a given delay, τ, and as g varies from 0 to ∞, it is obvious that the roots of equation (2) move from stable left half to the unstable right half of the complex plane. For a certain critical gain g_c one pair of poles reaches the imaginary axis. At this operating point, the DR is a perfect resonator, and the imaginary characteristic roots are $s = \pm \mathrm{j}\omega_c$, where ω_c is the resonance frequency and $\mathrm{j} = \sqrt{-1}$. The subscript c implies the crossing of the root loci on the imaginary axis. The control parameters g_c and τ_c of concern can be found by substituting the desired $s = \pm \mathrm{j}\omega_c$ into equation (2) as

$$g_c = (1/\omega_c^2)\sqrt{(c_a \omega_c)^2 + (m_a \omega_c^2 - k_a)^2}, \tag{5}$$

$$\tau_c = (1/\omega_c)\{\tan^{-1}[c_a \omega_c/(m_a \omega_c^2 - k_a)] + 2(\ell - 1)\pi\}, \quad \ell = 1, 2, \ldots. \tag{6}$$

When these g_c and τ_c are used the DR structure (Figure 1(b)) mimics a resonator at frequency ω_c. In turn this resonator forms an ideal absorber of tonal oscillations at ω_c. Returning to the distribution of roots, for $g > g_c$ the dominant roots move to the unstable right half of the complex plane, and therefore, render the DR structure unstable. The objective of the control is to maintain the DR absorber at this marginally stable point. On the DR stability, further discussions can be found in references [3, 5].

3. MULTIPLE IDENTICAL DR'S AS VIBRATION ABSORBERS FOR MDOF STRUCTURES

Multiple DR's are considered to suppress structural oscillations at several locations on a MDOF primary system. If the excitation were simple harmonic, the tuned DR absorbers could enforce artificial nodes at their points of attachment. There are a number of practical motivations for this: e.g., excited

large plates with sensitive devices at discrete locations; beams with similar vibration elimination requirements.

Several design considerations emanate on this basic proposition, mainly on the selection of the DR's structural properties (m_a, c_a, and k_a). If they were different for each DR (non-identical DR's) then the tuning gains and delays to the same excitation frequency (ω_c) would also be different as per equations (5) and (6). This brings a major difficulty in the stability analysis, due to the *presence of multiple unrelated delay* elements in the system. As a remedy identical DR absorbers are proposed. Notice two critical aspects: (1) when tuned to the only excitation frequency (ω_c), these absorbers use the same g and τ; (2) this tuning effort is not influenced by the primary MDOF system (see equations (5) and (6)). Inversely, there are no structural constraints on the MDOF primary relevant to the tuning. Even this identical DR case, however, yields some cumbersome mathematics when the system stability is studied as described in the following sections.

3.1. THE GOVERNING EQUATIONS

Attached to a general n-DOF system under harmonic excitation, r identical DR's ($r \leqslant n$) are considered. Each DR is properly tuned to the excitation frequency ω. They eliminate the oscillation of the primary structure at the points of attachment, creating distributed artificial nodes along the primary. A typical system is depicted in Figure 2.

The state-space representation of the system dynamics is written in the form:

$$\dot{\mathbf{y}}(t) = \mathbf{A}_0\mathbf{y}(t) + g\mathbf{A}_\tau\dot{\mathbf{y}}(t - \tau) + \mathbf{f}(t), \tag{7}$$

where

$$\mathbf{y}(t) = \{\underbrace{x_{a1}, \dot{x}_{a1}, \ldots, x_{ar}, \dot{x}_{ar}}_{2r}, \underbrace{x_1, \dot{x}_1, \ldots, x_n, \dot{x}_n}_{2n}\}^{\mathrm{T}},$$

$$\mathbf{f}(t) = \{\underbrace{0, \ldots, 0}_{2r}, \underbrace{0, f_1, 0, f_2, \ldots, 0, f_n}_{2n}\}^{\mathrm{T}} \in \mathcal{R}^{2(n+r) \times 1}$$

are the state variable and excitation vectors. The elastic deflections of the primary structure and absorbers are denoted by $x_i(t)$, $i = 1, \ldots, n$ and $x_{aj}(t)$, $j = 1, 2, \ldots, r$, respectively. $\mathbf{A}_0$ and $\mathbf{A}_\tau \in \mathcal{R}^{2(n+r) \times 2(n+r)}$ are the corresponding system matrices, τ and g are the identical time delays and feedback gains for all DR's.

The Laplace transform of equation (7) is

$$(s\mathbf{I} - \mathbf{A}_0 - gs\,\mathrm{e}^{-\tau s}\mathbf{A}_\tau)\mathbf{Y}(s) = \mathbf{F}(s) \Rightarrow \mathbf{H}(s, g, \tau)\mathbf{Y}(s) = \mathbf{F}(s). \tag{8}$$

The state vector $\mathbf{y}(t)$ can be obtained utilizing the inverse Laplace transform. Note that the terms of matrix $\mathbf{H}(s, g, \tau)$ in equation (8) not rational functions of s but transcendental, unlike the case of a non-delayed system. The poles of the system are those (complex) values of s for which $|\mathbf{H}|$ is zero. For non-delayed systems, i.e., when $g = 0$, these poles are the eigenvalues of the system matrix $\mathbf{A}_0$,
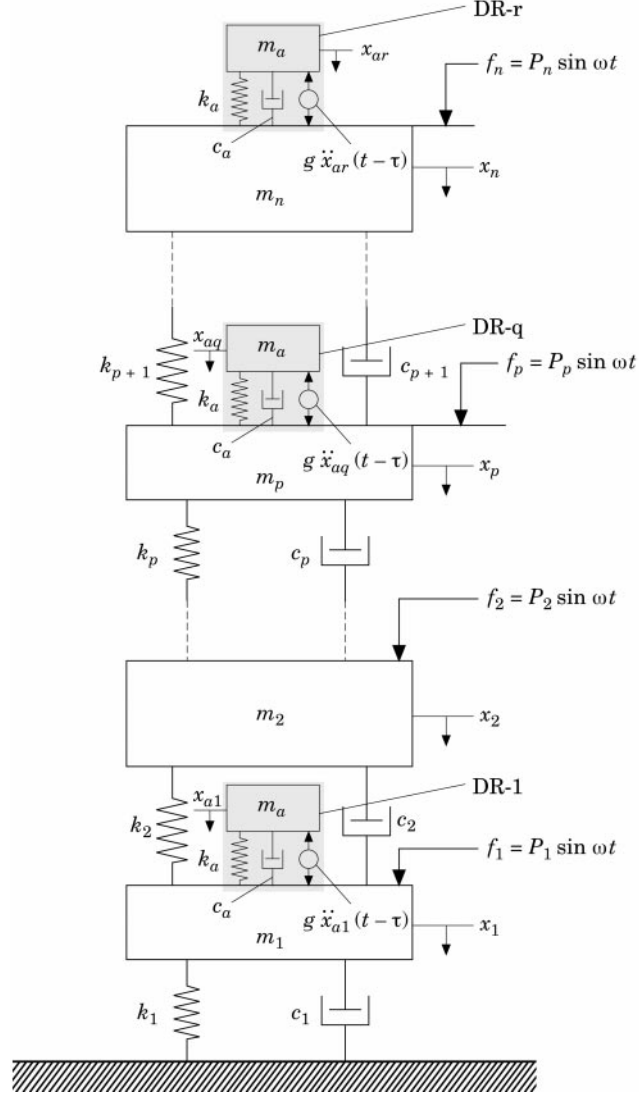
Figure 2. Configuration of the multiple Delayed Resonator absorbers for multi-degree-of-freedom structures.

i.e.,

$$\det(s\mathbf{I} - \mathbf{A}_0) = 0. \tag{9}$$

For the time-delayed system, however, equation (9) is augmented as

$$Q(s, g, \tau) = \det[s(\mathbf{I} - g\,\mathrm{e}^{-\tau s}\mathbf{A}_\tau) - \mathbf{A}_0] = 0. \tag{10}$$

Equation (10) has infinite number of roots, namely the *spectrum* of the time-delayed system.

The system of equations (8) can be rewritten in the explicit form

$$
\begin{pmatrix}
h_{11} & h_{12} & \cdots & h_{1\,2(n+r)} \\
h_{21} & h_{22} & \cdots & h_{2\,2(n+r)} \\
\vdots & \vdots & \vdots & \vdots \\
h_{2(n+r)\,1} & h_{2(n+r)\,2} & \cdots & h_{2(n+r)\,2(n+r)}
\end{pmatrix}
\begin{Bmatrix}
X_{a1}(s) \\
\vdots \\
X_{aq}(s) \\
\vdots \\
X_1(s) \\
\vdots \\
X_p(s) \\
\vdots
\end{Bmatrix}_{2(n+r)\times 1}
=
\begin{Bmatrix}
\mathbf{0}_{2r\times 1} \\
0 \\
F_1(s) \\
\vdots \\
0 \\
F_n(s)
\end{Bmatrix}_{2(n+r)\times 1}
, \quad (11)
$$

where $\{h_{ij}(s,\,g,\,\tau)\} = \mathbf{H}(s,\,g,\,\tau)$. It is shown that the displacement of the primary structure at the pth mass location can be determined utilizing Cramer's rule [5]:

$$
x_p(t) = \mathcal{L}^{-1}\{X_p(s)\} = \mathcal{L}^{-1}\left\{ \frac{(m_a s^2 + c_a s + k_a - g s^2\,\mathrm{e}^{-\tau s}) G_p(s,\,g,\,\tau)}{Q(s,\,g,\,\tau)} \right\}, \quad (12)
$$

where G_p is a function of s, the driving forces, and all the delay terms except the one corresponding to qth absorber which is attached to pth mass, and Q is defined in equation (10). Equation (12) implies that for a properly tuned DR, the primary structure should exhibit no oscillatory motion at location p. Notice that the characteristic equation (2) is a factor of the numerator in equation (12), and it is forced to be zero for $s = \pm\mathrm{j}\omega_c$ if g and τ are selected as in equations (5) and (6). These control parameters are functions of the frequency of excitation and properties of the absorber structure itself. That is, the control logic does not require any information from the primary structure, thus they are decoupled.

3.2. STABILITY ANALYSIS OF THE COMBINED SYSTEM

The stability is an important property of any feedback control system. For a system with variable time delay, stability analysis is relatively more difficult due to the transcendental terms in the characteristic equation.

The sufficient and necessary condition for asymptotic stability is that the roots of the transcendental characteristics equation (10) have negative real parts. The verification of the root locations, however, is not a trivial task. There are some fundamental methods suitable for such problems: e.g. Root-Locus, Nyquist, Michailov and Pontryagin criteria [10–15]. One makes a qualitative remark here that none of these methods is suitable for multiple time delay cases.

It is easy to show from the characteristic equation (10) that the delay terms in the characteristic equation appear in the form of $\mathrm{e}^{-k\tau s}$, $k \leqslant r$. Delays such as these, which are integer multiples of a single delay τ, are called commensurate delays [16]. Even in this relatively simple case, the stability problem is not a straightforward task to handle, as explained later in the text.

The characteristic equation (10) can be written in a simplified form as

$$\sum_{k=0}^{r} H_k(s)g^k \, e^{-k\tau s} = 0. \tag{13}$$

In the most general case, all these commensurate delay terms $e^{-\tau s} \cdots e^{-r\tau s}$ are present in the characteristic equation (13). A "*peeling-off*" procedure is adopted to eliminate the highest order delay terms in this equation [16]. This reduces the problem of commensurate delays to the one with single delay. Following is a brief explanation of this procedure. Equation (13) is rewritten as

$$H_0(s) + H_1(s)g \, e^{-\tau s} + \cdots + H_r(s)g^r \, e^{-r\tau s} = 0. \tag{14}$$

one is interested in the purely imaginary solutions of this equation to find out the marginal stability bounds. For such roots, s, $-s$ (i.e., the complex conjugate of s) must also be a root. Hence, substituting $-s$ into this equation one obtains

$$H_0 + H_1 g \, e^{-\tau s} + \cdots + H_r g^r \, e^{-r\tau s} = 0, \quad \bar{H}_0 + \bar{H}_1 g \, e^{\tau s} + \cdots + \bar{H}_r g^r \, e^{r\tau s} = 0, \tag{15}$$

where

$$\bar{H}_0 = H_0(-s), \quad \bar{H}_1 = H_1(-s), \ldots, \bar{H}_r = H_r(-s). \tag{16}$$

The second equation (15) is multiplied by $e^{-r\tau s}$, solved for $e^{-r\tau s}$ substitute which is into the first equation. This eliminates the highest order term, $e^{-r\tau s}$, and yields

$$(g^{2r} H_r \bar{H}_r - H_0 \bar{H}_0) + (g^{2r-2} H_r \bar{H}_{r-1} - H_1 \bar{H}_0)g \, e^{-\tau s} + \cdots$$
$$+ (g^2 H_r \bar{H}_1 - H_{r-1} \bar{H}_0)g^{r-1} \, e^{-(r-1)\tau s} = 0. \tag{17}$$

Successive elimination of $e^{-(r-1)\tau s}$, $e^{-(r-2)\tau s}, \ldots,$ $e^{-2\tau s}$ terms in equation (17) recasts the characteristic equation in its most general form as

$$M(g, s) + N(g, s)g \, e^{-\tau s} = 0, \tag{18}$$

where M and N are polynomials of s with respective degrees of α and β and functions of feedback gain g. A case study for this procedure is presented in the simulations section for clarity.

When the combined system is marginally stable, there are at least two roots on the imaginary axis, i.e., $s = \pm j\omega_{cs}$. Enforcing this into equation (18) yields the delay and feedback values that make the combined system marginally stable as

$$g_{cs} = \| M(g_{cs}, j\omega_{cs})/N(g_{cs}, j\omega_{cs}) \|, \tag{19}$$

$$\tau_{cs} = 1/\omega_{cs} \left\{ (2\ell - 1)\pi - \angle \frac{M(g_{cs}, j\omega_{cs})}{N(g_{cs}, j\omega_{cs})} \right\} \ell = 1, 2 \ldots, \tag{20}$$

where $\angle$ denotes the angle of the argument. Note that equation (19) is an implicit equation in terms of g_{cs}, and could have multiple solutions.

One utilizes the stability analysis of section 2 for the DR alone, on the combined system. An equation for the magnitude is obtained as

$$g = (\| M(g, s) \|_{s=a+j\omega} / \| N(s, g) \|_{s=a+j\omega}) e^{\tau a}, \qquad (21)$$

where $a = \mathcal{R}e(s)$. From equation (21), it is easy to evaluate that for $g = 0$, there are α stable poles which are the roots of polynomial $M(s)$ (or simply the eigenvalues of the uncontrolled system matrix $\mathbf{A}_0$) while all other roots are at $a = -\infty$. As $g \to +\infty$, β poles approach the roots of $N(s)$ and the rest tend to $\mathcal{R}e(s) = +\infty$.

Thus, increasing feedback gain, g, from 0 to $+\infty$ while the time delay τ is kept constant, drives the combined system through the stable, marginally stable, and ultimately to the unstable behavior. For a particular delay $\tau = \tau_0$, the combined system crossings, $\omega_{csi}(\tau_0)$ are determined from equation (20) and corresponding gains, g_{csi}, from equation (19), where the subscript $i = 1, 2, \ldots$ refers to the first, second, etc., crossings. To ensure stability of the system, the feedback gain g should be smaller than the infemum of these $g_{csi}(\omega_{csi})$ values. That is,

$$g < g_{min}(\omega_{csi}(\tau_0)), \qquad (22)$$

where

$$g_{min} = \text{infemum} \left\{ \begin{array}{c} g_{cs}(\omega_{cs1}) \\ g_{cs}(\omega_{cs2}) \\ g_{cs}(\omega_{cs3}) \end{array} \right\}, \quad \text{for} \quad \tau = \tau_0. \qquad (23)$$

The plot of $g_{min}(\omega_{cs})$ versus $\tau_{cs}(\omega_{cs})$ is, therefore, the lower envelope of the parameterized stability plot of the combined system, $g_{cs}(\omega_{cs})$ versus $\tau_{cs}(\omega_{cs})$. This envelope is numerically obtained for each "m_a, c_a, k_a" set of absorber parameters. The procedure is explained in detail in section 5.

The ratio of the combined system gain and DR gain $(g_{cs}(\tau)/g_c(\tau))$ can be defined as the "*stability margin*" of the control system, at the particular delay value τ. The comparison of the $g_{cs}(\omega_c)$ versus $\tau_{cs}(\omega_c)$ plot of the combined system with the $g_c(\omega_c)$ versus $\tau_c(\omega_c)$ plot of the DR reveals this stability margin for the entire frequency spectrum. This picture also yields the frequency range for the stable operation of the combined system. That is, for a given τ_c the system is stable if $g_c < g_{cs}$ or the stability margin is greater than one. An example of such treatment is also presented in the simulations section.

4. PARAMETRIC INFLUENCE OF DESIGN SELECTION ON THE ABSORPTION PERFORMANCE

An interesting question for a multiple DR application is the absorber tuning speed when the excitation frequency varies. This feature is critical because it represents the frequency tracking ability of the absorber. It is dictated by the dominant characteristic roots of the system. For a given primary structure $(m_i, k_i, c_i, \ i = 1, 2, \ldots, n)$, the DR's parameters (m_a, k_a, c_a) should be selected such that the dominant roots of the characteristic equation (13) are appropriately positioned.

Due to the transcendental nature of this characteristic equation, an analytical approach is impossible. To resolve this, a practical implementation of Nyquist criterion, as described below, is adopted from reference [4].

First, the Bromwich contour, encompassing the right half of the complex plane, is traced for the $\mathcal{R}e(s) > 0$ semi-infinite domain, yielding no roots within the contour (i.e., stable system). Next, the imaginary axis is shifted using $\bar{s} = s + a$, $a \in \mathcal{R}^+$ and the Nyquist search for $\mathcal{R}e(\bar{s}) > 0$ semi-infinite space is repeated. This numerical search is performed for increasing values of a. When the right-most characteristic roots are encountered in $a = a_0 - \varepsilon$ to $a = a_0 + \varepsilon$ transition, where $\varepsilon \in \mathcal{R}^+$ and $\varepsilon \ll 1$, the Nyquist criterion flags a switch from no roots to some roots, respectively. This implies that the dominant roots fall in the interval $-(a_0 + \varepsilon) < \mathcal{R}e(s) < -(a_0 - \varepsilon)$.

The transient behavior of the combined system is dictated by this dominant pole. That is, the system exhibits a decay with a time constant of $1/a_0$. The dynamics manifest a steady state within approximately four time constants $(4/a_0)$. For the given absorber(s) m_a, k_a, c_a, the system reacts with this tuning speed. If this current setting is not satisfactory, alternate design parameters should be tested. Notice that larger stability margin (of section 3.2) yields faster tuning. This feature could be used as a design tool to improve the tuning speed. This issue is explained further in section 5.

5. DYNAMIC SIMULATIONS AND RESULTS

To demonstrate the validity of using multiple DR's, a combination of two identical DR's on a 3-DOF structure is studied (Figure 3). The system is excited by a simple harmonic force at m_2 location on the primary structure. The objective is to eliminate the vibration of the other two masses, i.e., m_1 and m_3. This is achieved by applying two DR's attached to these masses. The numerical values for the primary structure are taken as: $m_1 = m_3 = 10$ and $m_2 = 50$ kg; $k_1 = k_3 = 1$ and $k_2 = 2$ kN/m; $c_1 = c_3 = 20$ and $c_2 = 25$ Ns/m. This selection is made for demonstration purposes only and has no direct practical correspondence.

The state-space representation of the system is

$$\dot{\mathbf{y}}(t) = \mathbf{A}_0 \mathbf{y}(t) + g\mathbf{A}_\tau \dot{\mathbf{y}}(t - \tau) + \mathbf{f}(t), \tag{24}$$

The matrices $\mathbf{A}_0$ and $\mathbf{A}_\tau$ are defined in Appendix A. $\mathbf{f}(t) = \{0, 0, 0, 0, 0, 0, 0, f, 0, 0\}^T$ and $\mathbf{y}(t) = \{x_{a1}, \dot{x}_{a1}, x_{a2}, \dot{x}_{a2}, x_1, \dot{x}_1, x_2, \dot{x}_2, x_3, \dot{x}_3\}^T$ are the force and state vectors, respectively. In this case the characteristic equation is

$$H_0(s) + H_1(s)g\, e^{-\tau s} + H_2(s)g^2\, e^{-2\tau s} = 0, \tag{25}$$

where $H_0(s)$, $H_1(s)$, and $H_2(s)$ are polynomials of s with real coefficients presented in Appendix A.

The "*peeling-off*" method is used to eliminate $e^{-2\tau s}$ term first. For this, the system of equations

$$H_0 + H_1 g\, e^{-\tau s} + H_2 g^2\, e^{-2\tau s} = 0, \quad \bar{H}_0 + \bar{H}_1 g\, e^{\tau s} + \bar{H}_2 g^2\, e^{2\tau s} = 0 \tag{26}$$
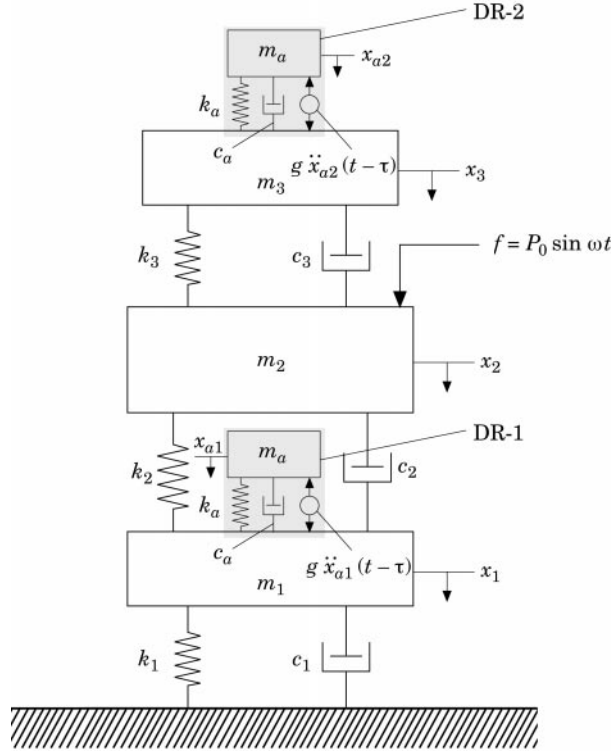
Figure 3. A generic case of two identical DR implementation on a 3-DOF structure.

is solved to eliminate $e^{-2\tau s}$. This process yields

$$g\, e^{-\tau s} = (\bar{H}_0 H_0 - g^4 \bar{H}_2 H_2)/(g^2 \bar{H}_1 H_2 - H_1 \bar{H}_0). \tag{27}$$

When the combined system is marginally stable, there are at least two roots of the characteristic equation on the imaginary axis, i.e., $s = \pm j\omega_{cs}$. Introducing this condition into equation (27), gives the delay and gain values that make the combined system marginally stable as

$$g_{cs} = \left\| \frac{\bar{H}_0(s)H_0(s) - g_{cs}^4 \bar{H}_2(s)H_2(s)}{g_{cs}^2 \bar{H}_1(s)H_2(s) - H_1(s)\bar{H}_0(s)} \right\|_{s=j\omega_{cs}},$$

$$\tau_{cs} = (1/\omega_{cs})\{(2\ell-1)\pi + \angle[g_{cs}^2 \bar{H}_1(s)H_2(s) - H_1(s)\bar{H}_0(s)]_{s=j\omega_{cs}}\}\ \ell = 1, 2, \ldots. \tag{28}$$

From equation (28) an important observation is that the feedback gain cannot be determined explicitly for multiple DR cases. This is a major difference between the single and multiple DR cases. Notice that equation (25) has $H_2(s) = 0$ for single usage of DR. In this case, equation (28) reflects an explicit expression for g_{cs}, which was reported earlier [7].

The $g_{cs}(\omega_{cs})$ versus $\tau_{cs}(\omega_{cs})$ plots for the given system are generated using equation (28). The following procedure is used: (1) An interval of ω_{cs} is taken

say (5 ⋯ 100 rad/s); (2) the g_{cs} values which satisfy the first equation in (28) for an ω_{cs} are numerically calculated; (3) for a g_{cs} and the corresponding ω_{cs}, the second equation (28) yields a τ_{cs}. Notice that τ_{cs} is also multivalued due to the crossing root loci identifier $\ell (= 1, 2, \ldots)$.

The lower envelop points of the operating points, $\{g_{cs}, \tau_{cs}\}$, $\ell = 1, 2, \ldots$, form the marginal stability boundary for the combined system. For a lower value of g_{cs} below this envelop, i.e., $g_{cs} <$ infemum $(g_{cs}(\tau_{cs}))$, the system is stable. For higher values, it is unstable. This judgment follows the "D-subdivision" principle explained in references [8, 17] and applied for DR stability analysis in reference [18]. Note that the $g = 0$ (no feedback) line lies always in the stable zone.

These stability boundaries (which are alternatively known as the "stability chart") are depicted in Figure 4(a) (by solid lines). The reasons for the jagged appearance are: (1) the equally spaced ω_{cs} variation does not yield a smooth spacing in τ_{cs}; (2) the g_{cs} versus τ_{cs} curves exhibit looping outlook as explained in reference [5]. This gives rise to the spikes such as points A and B.

For this plot the absorber s structural parameters are taken as: $m_a = 1$ kg, $k_a = 100$ N/m, and $c_a = 0 \cdot 1$ Ns/m. Note that this selection suggests a 1/35 mass ratio for the absorber.

The comparison of the stability charts of the combined system and of the DR reveals a stable frequency range for the absorption. Please note that for ideal suppression the control maintains the DR on the stability border (dotted lines in Figure 4(a)). These operating points should be in the stable operating zones of the combined system. This condition yields stable operations in some ranges of τ, such as $0 \cdot 52 < \tau < 0 \cdot 94$ s, on the second root loci branch ($\ell = 2$).

Figure 4(b) depicts the correspondence between the delay τ, and the frequency ω_c of absorption. For instance, the stable interval of τ given as example above, corresponds to $9 \cdot 5 < \omega_c < 12$ rad/s.

This procedure can be used as a design tool for selecting the DR parameters (m_a, k_a, c_a). If, for instance, the excitation frequency falls outside a stable (operable) frequency range, m_a, k_a, c_a can be altered until the satisfactory stability picture is reached. A parametric sensitivity analysis can also be considered as an extension to this work.

Figure 4 contains the stability charts, which show the majority of the operating points fall in the stable territory. However, the stability margin is not large, and therefore the absorption transients are long. It should be noted that the stability margin is, indeed, an indication of the location of the dominant roots of the combined system. As proven earlier for single DR cases, the smaller the stability margin the closer the dominant roots to the imaginary axis, and therefore the longer the settling time [8, 14, 15]. This feature is shown next using simulation examples.

For the above selection of primary system and DR absorbers settings, the eigenvalues of the uncontrolled ($g = 0$) combined system are found as

$$s_{1,2} = -0 \cdot 0856 \pm j9 \cdot 8940, \quad s_{3,4} = -0 \cdot 0881 \pm j3 \cdot 1393, \quad s_{5,6} = -0 \cdot 3673 \pm j9 \cdot 1440,$$

$$s_{7,8} = -0 \cdot 8774 \pm j11 \cdot 9799, \quad s_{9,10} = -2 \cdot 3915 \pm j18 \cdot 3604, \tag{29}$$
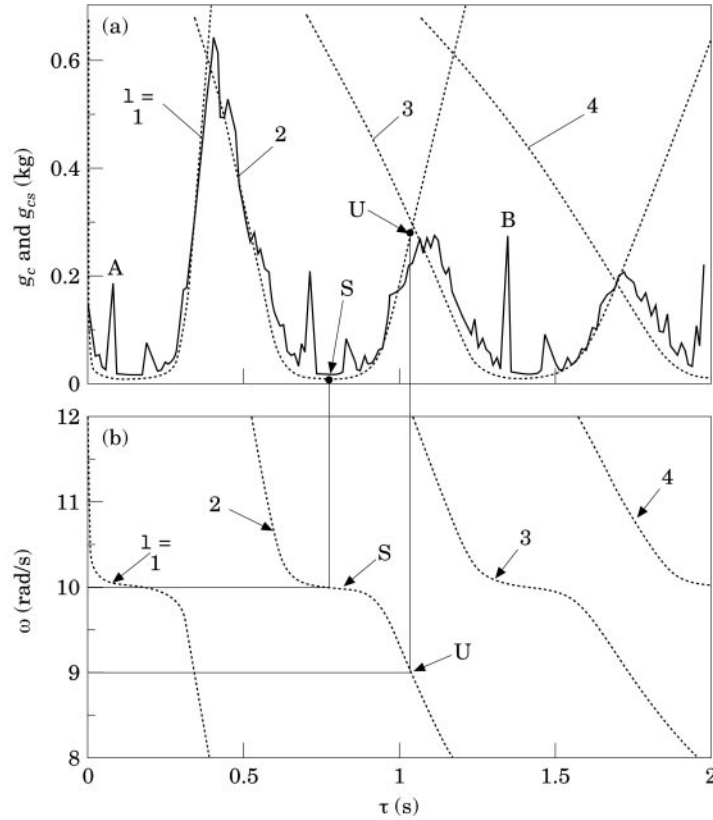
Figure 4. (a) Stability charts: plot of gain vs. time delay for both combined system and DR, (b) plot of excitation frequency vs. time delay for DR alone; · · · · , DR absorbers alone; —, combined system; ●, example operations.

which means the real part of the dominant roots is at -0.0856 (implying a transient behavior of approximately 50 s), and the system natural frequencies are roughly

$$3, 9, 10, 12, 19 \text{ rad/s}. \tag{30}$$

In order to verify the validity of the stability zones found in Figure 4, one selects two operating points. One excitation frequency is selected to be in the stable, and the other in the unstable zones. Figure 5 shows a test with the excitation frequency $\omega_c = 10$ rad/s, which corresponds to one of the system resonance frequencies (point **S** in Figure 4, stable operation). The DR tuning parameters are $g_c = 0.014$ kg and $\tau_c = 0.7854$ s for this frequency. The displacements of the primary structure at the points of attachment of the two DR's decay exponentially, as shown in Figures 5(a) and (c). Figures 5(d) and (e) display the absorber responses. The suppression takes effect in approximately 100 s. Using Nyquist method, the real part of dominant roots is found in the interval $-0.04 < -a_0 < -0.03$ which corresponds to the settling time
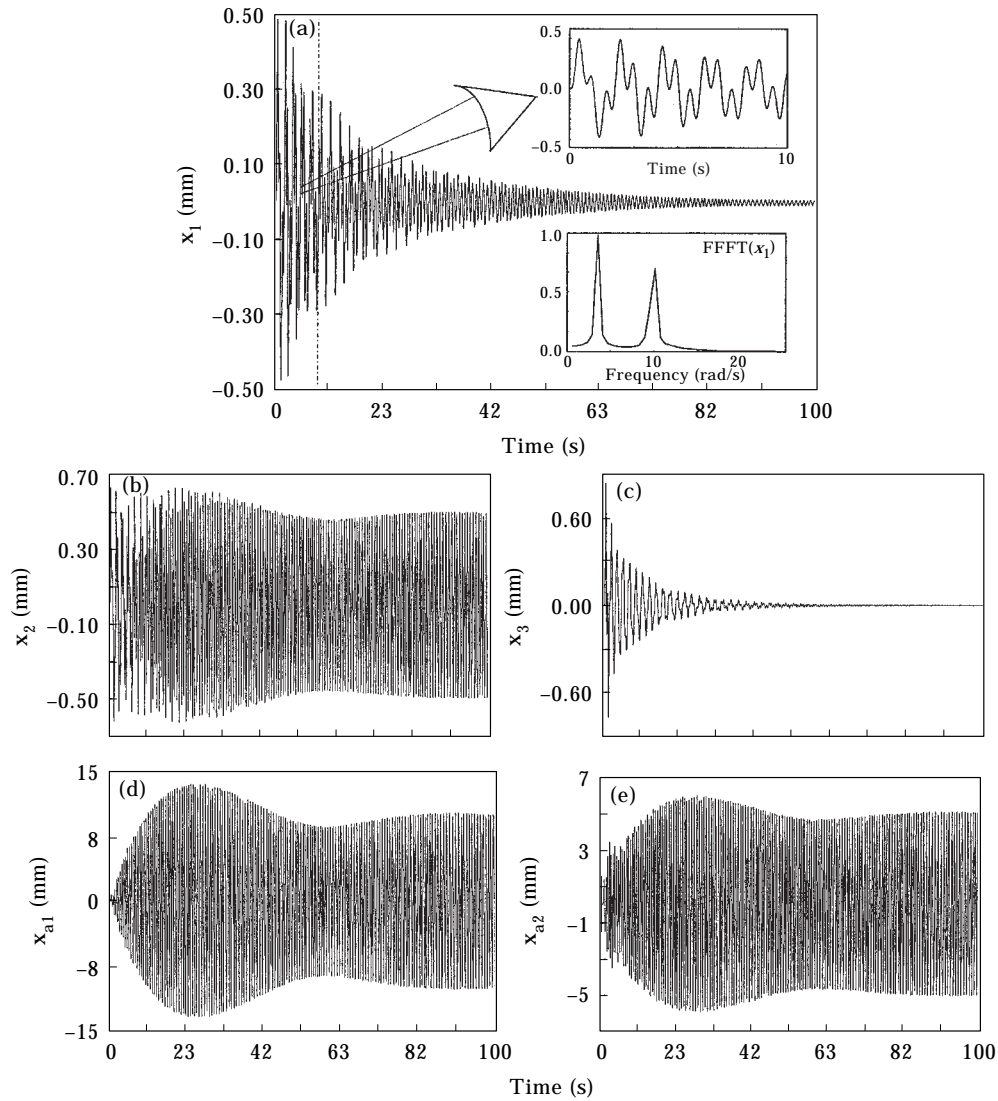
Figure 5. The time traces of system s response for the stable excitation frequency $\omega_c = 10$ rad/s (point "**S**" in Figure 4): (a) absorber 1 point of attachment (m_1), (b) excitation location (m_2), (c) absorber 2 point of attachment (m_3), (d) absorber 1 (m_a), (e) absorber 2 (m_a).

of $100 < t_s < 130$ s. The time trace of x_1 is exploded for the first 10 s just to highlight that there exists a low frequency component (Figure 5(a)). A Fast Fourier Transform (FFT) is also given for this trace showing spectral peaks at approximately 3·8 and 10 rad/s. The second peak is due to the excitation (i.e., the forced response), but the first one corresponds to one of the system modes which is lightly damped. For this operating point a system pole is located very close to $\pm$j3·8. This pole is the relocated form of $s_{3,4}$ of equation (29) under the
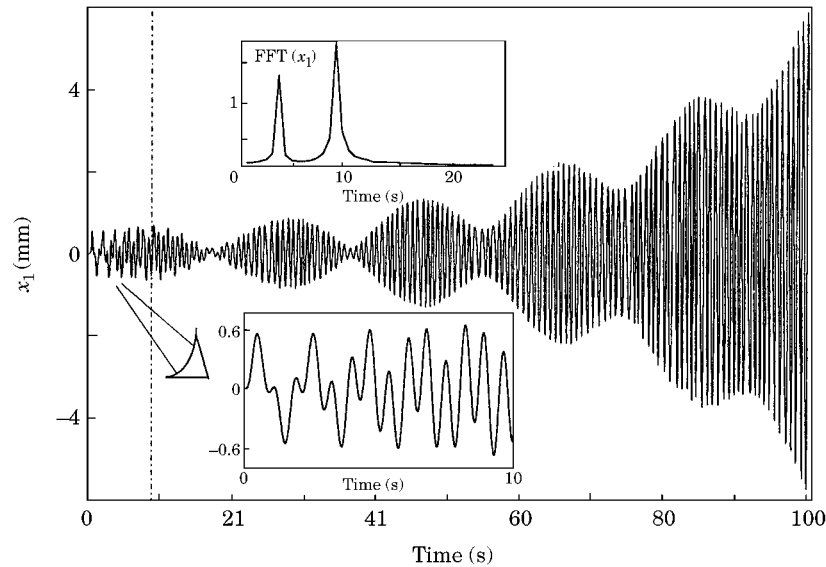
Figure 6. The time trace of point of attachment of absorber 1 (x_1), for the unstable excitation frequency $\omega_c = 9$ rad/s (point "**U**" in Figure 4).

feedback. Both the excitation and the modal frequency vibrations are suppressed later on.

Next, an unstable operating point is tested, **U** in Figure 4, which corresponds to the excitation frequency $\omega_c = 9$ rad/s and again one of the system resonance frequencies. The DR control parameters are $g_c = 0.2348$ kg and $\tau_c = 1.0419$ s. Figure 6 shows the time response of $x_1(t)$ only. The displacements are oscillatory but with amplitudes which increase exponentially. Obviously, this DR is not usable for absorption at this frequency. The FFT of the first 10 s trace shows, again, similar spectral peaks: 3·8 rad/s (system modal frequency) and 9 rad/s (excitation). Notice that the relocated pole is again very close to $\pm j3·8$, by coincidence.

6. CONCLUSIONS

The use of multiple DR absorbers is a viable technique to suppress tonal oscillations completely at several locations on MDOF mechanical structures. The stability of the entire system is addressed utilizing a stability chart strategy. A *peeling-off* procedure is presented to simplify the stability assessment by converting the problem of multiple DR's to a single delay representation. The agreement between stability charts and simulated time responses is shown via numerical examples. The stability margins and tuning times are observed from these simulations.

The issues presented in this paper on the use of multiple DR's lend themselves to further investigation. The following problems are currently being studied: (1) multiple unrelated DR vibration absorbers utilized on MDOF structures against multi-frequency excitations; (2) optimization algorithm for designing the DR's parameters in order to improve absorption performance.

ACKNOWLEDGMENTS

REFERENCES

1. N. OLGAC 1995 *U.S. Patent* 5,431,261. Delayed resonators as active dynamic absorbers.
2. N. OLGAC and B. HOLM-HANSEN 1994 *Journal of Sound and Vibration* **176**, 93–104. A novel active vibration absorption technique: delayed resonator.
3. N. OLGAC and B. HOLM-HANSEN 1995 *ASME Journal of Dynamic Systems, Measurement, and Control* **117**, 513–519. Tunable active vibration absorber: the delayed resonator.
4. N. OLGAC and B. HOLM-HANSEN 1995 *Journal of Engineering Mechanics* **121**, 80–89. Design considerations for delayed-resonator vibration absorbers.
5. N. OLGAC, H. ELMALI, M. HOSEK and M. RENZULLI 1997 *ASME Journal of Dynamic Systems, Measurement, and Control* **119**, 380–389. Active vibration control of distributed systems using delayed resonator with acceleration feedback.
6. M. RENZULLI, R. GHOSH-ROY and N. OLGAC 1997 *Proceedings of Third ARO Workshop on Smart Structures*. Robust control of the delayed resonator vibration absorbers.
7. N. OLGAC and N. JALILI 1998, *Journal of Sound and Vibration* **218**, 307–331. Modal analysis of flexible beams with delayed resonator vibration absorber: theory and experiment.
8. V. B. KOLMANOVSKI and V. R. NOSOV 1989 *Stability of Functional Differential Equations*. London: Academic Press.
9. K. YOUCEF-TOUMI and J. BOBBETT 1991 *ASME Journal of Dynamic Systems, Measurement, and Control* **113**, 558–567. Stability of uncertain linear systems with time delay.
10. A. THOWSEN 1982 *IEE Proceedings* **29**, 73–75. Delay-independent asymptotic stability of linear systems.
11. D. HERTZ, E. I. JURY and E. ZEHEB 1984 *IEE Proceedings* **131** (D), 52–56. Simplified analytic stability test for systems with commensurate time delays.
12. L. PONTRYAGIN 1955 *Transaction of American Mathematics Society* **2**, 95–110. On the zeros of some elementary transcendental functions.
13. E. P. POPOV 1962 *The Dynamics of Automatic Control Systems*. Oxford: Pergamon Press.
14. A. M. KRALL 1967 *Stability Techniques for Continuous Linear Systems*. New York, Gordon & Breach.

15. G. STEPAN 1989 *Retarded Dynamical Systems: Stability and Characteristic Functions*. London: Longman Scientific and Technical. Pitman research notes in mathematics series.
16. K. WALTON and J. E. MARSHALL 1987 *Proceeding of the IEE* **134** (D), 101–107. A direct method for TDS stability analysis.
17. J. ACKERMANN 1993 *Robust Control*, *Systems with Uncertain Physical Parameters*. Berlin, Springer.
18. D. FILIPOVIC and N. OLGAC 1998 *IEEE/ASME Transaction on Mechatronics* **3**, 67–72. Torsional delayed resonator with velocity feedback.

A.1. COEFFICIENT MATRIX IN EQUATION (24)

$$\mathbf{A}_0 = \begin{bmatrix}
0 & 1 & 0 & 0 & 0 & 0 & 0 & 0 & 0 & 0 \\[4pt]
\dfrac{-k_a}{m_a} & \dfrac{-c_a}{m_a} & 0 & 0 & \dfrac{k_a}{m_a} & \dfrac{c_a}{m_a} & 0 & 0 & 0 & 0 \\[8pt]
0 & 0 & 0 & 1 & 0 & 0 & 0 & 0 & 0 & 0 \\[4pt]
0 & 0 & \dfrac{-k_a}{m_a} & \dfrac{-c_a}{m_a} & 0 & 0 & 0 & 0 & \dfrac{k_a}{m_a} & \dfrac{c_a}{m_a} \\[8pt]
0 & 0 & 0 & 0 & 0 & 1 & 0 & 0 & 0 & 0 \\[4pt]
\dfrac{k_a}{m_1} & \dfrac{c_a}{m_1} & 0 & 0 & \dfrac{-(k_1+k_2+k_a)}{m_1} & \dfrac{-(c_1+c_2+c_a)}{m_1} & \dfrac{k_2}{m_1} & \dfrac{c_2}{m_1} & 0 & 0 \\[8pt]
0 & 0 & 0 & 0 & 0 & 0 & 0 & 1 & 0 & 0 \\[4pt]
0 & 0 & 0 & 0 & \dfrac{k_2}{m_2} & \dfrac{c_2}{m_2} & \dfrac{-(k_2+k_3)}{m_2} & \dfrac{-(c_2+c_3)}{m_2} & \dfrac{k_3}{m_2} & \dfrac{c_3}{m_2} \\[8pt]
0 & 0 & 0 & 0 & 0 & 0 & 0 & 0 & 0 & 1 \\[4pt]
0 & 0 & \dfrac{k_a}{m_3} & \dfrac{c_a}{m_3} & 0 & 0 & \dfrac{k_3}{m_3} & \dfrac{c_3}{m_3} & \dfrac{-(k_3+k_a)}{m_3} & \dfrac{-(c_3+c_a)}{m_3}
\end{bmatrix}_{10\times10},$$

$$\mathbf{A}_\tau = \begin{bmatrix} 0 & 0 & 0 & 0 & 0 & 0 & 0 & 0 & 0 & 0 \\ 0 & 1/m_a & 0 & 0 & 0 & 0 & 0 & 0 & 0 & 0 \\ 0 & 0 & 0 & 0 & 0 & 0 & 0 & 0 & 0 & 0 \\ 0 & 0 & 0 & 1/m_a & 0 & 0 & 0 & 0 & 0 & 0 \\ 0 & 0 & 0 & 0 & 0 & 0 & 0 & 0 & 0 & 0 \\ 0 & -1/m_1 & 0 & 0 & 0 & 0 & 0 & 0 & 0 & 0 \\ 0 & 0 & 0 & 0 & 0 & 0 & 0 & 0 & 0 & 0 \\ 0 & 0 & 0 & 0 & 0 & 0 & 0 & 0 & 0 & 0 \\ 0 & 0 & 0 & 0 & 0 & 0 & 0 & 0 & 0 & 0 \\ 0 & 0 & 0 & -1/m_3 & 0 & 0 & 0 & 0 & 0 & 0 \end{bmatrix}_{10 \times 10}.$$

A.2. COEFFICIENT POLYNOMIALS IN EQUATION (25)

$$
\begin{aligned}
H_0 =\ & c_a^2(u_2 c_a^2 + c_3^2 u_a + c_2^2 u_a)s^4 + 2c_a(2u_2 k_a c_a^2 + u_a c_a k_2 c_2 + u_a c_a k_3 c_3 \\
& + u_a c_2^2 k_a + u_a k_a c_3^2)s^3 + (-u_a^2 u_3 c_2^2 + u_a k_a^2 c_3^2 + u_a c_a^2 k_3^2 + 4u_a c_a k_a c_3 k_3 \\
& + 4u_a c_a k_a k_2 c_2 - u_a u_1 u_2 c_a^2 + u_a c_a^2 k_2^2 + u_a c_2^2 k_a^2 - u_a u_2 u_3 c_a^2 - u_a^2 u_1 c_3^2 + 6u_2 c_a^2 k_a^2)s^2 \\
& + (2u_a c_a k_a k_3^2 + 2u_a k_a^2 c_3 k_3 - 2u_a u_2 u_3 c_a k_a + 2u_a c_2 k_2 k_a^2 + 2u_a c_a k_2^2 k_a \\
& - 2u_a^2 u_3 c_2 k_2 - 2u_a u_1 u_2 c_a k_a - 2u_a^2 u_1 c_3 k_3 + 4u_2 c_a k_a^3)s + u_a^2 u_1 u_2 u_3 \\
& - u_a u_1 u_2 k_a^2 - u_a^2 u_1 k_3^2 + u_2 k_a^4 + u_a k_a^2 k_3^2 - u_a u_2 u_3 k_a^2 - u_a^2 u_3 k_2^2 + u_a k_2^2 k_a^2.
\end{aligned}
$$

$$
\begin{aligned}
H_1 =\ & -c_a^2(c_2^2 + c_3^2)s^6 - c_a(2u_2 c_a^2 + 2c_a k_2 c_2 + 2c_a k_3 c_3 + 2k_a c_2^2 \\
& + u_a c_2^2 + 2c_3^2 k_a + u_a c_3^2)s^5 + (-c_a^2 k_2^2 + u_1 u_2 c_a^2 - 2u_a c_a k_3 c_3 \\
& + 2u_a u_1 c_3^2 - 4c_a c_3 k_3 k_a + u_2 u_3 c_a^2 - k_a^2 c_3^2 - c_2^2 k_a^2 - c_a^2 k_3^2 - 6u_1 k_a c_a^2 \\
& + 2u_a u_3 c_2^2 - 4c_a c_2 k_2 k_a - u_a k_a c_3^2 - u_a c_2^2 k_a - 2u_a c_a k_2 c_2)s^4 + (-6u_2 c_a k_a^2 \\
& + 2u_1 u_2 c_a k_a + 4u_a u_3 c_2 k_2 + u_a u_2 u_3 c_a - 2k_a^2 c_3 k_3 - 2c_2 k_2 k_a^2 - 2c_a k_2^2 k_a \\
& - u_a c_a k_3^2 - u_a k_2^2 c_a + 4u_a u_1 c_3 k_3 - 2u_a k_a c_3 k_3 + 2u_2 u_3 c_a k_a + u_a u_1 u_2 c_a \\
& - 2u_a c_2 k_2 k_a - 2c_a k_a k_3^2)s^3 + (2u_a u_3 k_2^2 + u_2 u_3 k_a^2 + u_1 u_2 k_a^2 + u_a u_2 u_3 k_a \\
& + u_a u_1 u_2 k_a - k_2^2 k_a^2 - u_a k_2^2 k_a - 2u_2 k_a^3 + 2u_a u_1 k_3^2 - k_a^2 k_3^2 \\
& - 2u_a u_1 u_2 u_3 - u_a k_a k_3^2)s^2,
\end{aligned}
$$

$$H_2 = c_a(c_2^2 + c_3^2)s_7^2 + (k_ac_2^2 - u_3c_2^2 + u_2c_a^2 + 2c_ak_3c_3 + 2c_ak_2c_2 - u_1c_3^2 + c_3^2k_a)s^6$$

$$+ (2c_2k_2k_a + k_2^2c_a - 2u_1c_3k_3 - 2u_3c_2k_2 - u_2u_3c_a + 2k_ac_3k_3 + c_ak_3^2$$

$$+ 2u_2c_ak_a - u_1u_2c_a)s^5 + (u_1u_2u_3 + k_2^2k_a - u_2u_3k_a - u_1u_2k_a - u_3k_2^2$$

$$+ k_ak_3^2 - u_1k_3^2 + u_2k_a^2)s^4,$$

where

$$u_a = m_as^2 + c_as + k_a, \quad u_1 = m_1s^2 + (c_1 + c_2 + c_a)s + k_1 + k_2 + k_a,$$

$$u_2 = m_2s^2 + (c_2 + c_3)s + k_2 + k_3, \quad u_3 = m_3s^2 + (c_3 + c_a)s + k_3 + k_a.$$